Modulating interface performance between 2D semiconductor $MoSi_2N_4$ and its native high-*k* dielectric Si_3N_4

Jiahao Chen[1], Yang Zuo[1], Chin Yuan Ong[1], Jingyu He[1], Yulin Yang[2], Lai Mun Wong[3], Xiaoman Zhang[4, *], and Ming Yang[1, 5, 6, *]

[1] Department of Applied Physics, The Hong Kong Polytechnic University, Hung Hom, Hong Kong SAR, China

[2] Fujian Provincial Key Laboratory of Optoelectronic Technology and Devices, School of Optoelectronic and Communication Engineering, Xiamen University of Technology, Xiamen, 361024, China

[3] Institute of Materials Research and Engineering (IMRE), Agency for Science, Technology and Research (A*STAR), 2 Fusionopolis Way, Innovis #08-03, 138634, Republic of Singapore

[4] College of Photonic and Electronic Engineering, Fujian Normal University, Fuzhou, 35007, China

[5] Research Centre on Data Sciences & Artificial Intelligence, The Hong Kong Polytechnic University, Hung Hom, Hong Kong SAR, China

[6] Research Centre for Nanoscience and Nanotechnology, The Hong Kong Polytechnic University, Hung Hom, Hong Kong SAR, China

* Author to whom correspondence should be addressed: M.Y. (kevin.m.yang@polyu.edu.hk) or X.M.Z.(xmzhang@fjnu.edu.cn)

Abstract

Two-dimensional (2D) transition metal silicon nitride (MSi_2N_4: M denotes Mo or W) are promising channel materials for nanoelectronics owing to their attractive structural and electronic properties. The integration of high-κ dielectrics into 2D semiconductors MSi_2N_4 is one of the vital steps for achieving high-performance electronic devices, which however remains challenging. In this study, we propose silicon nitride (Si_3N_4) as the native high-κ dielectric for 2D MSi_2N_4 and reveal their interfacial properties. Using first-principles calculations, we show that a high-performance interface can be formed, as supported by weak interface interaction, insignificant charge density redistribution, and nearly intact electronic properties of monolayer MSi_2N_4 with the integration of Si_3N_4. We further demonstrate that interfacial hydrogenation can effectively passivate the dangling bonds at Si_3N_4 surface, leading to improved interface performance. Importantly, this interfacial hydrogenation does not bring detrimental effect to both the high-κ dielectric and the 2D semiconductors, as it is thermodynamically and kinetically stable at the Si_3N_4 surface. These results provide a deep understanding for the integration of high-κ dielectrics on 2D semiconductors MSi_2N_4, design a viable interfacial engineering strategy to improve the interface performance, and therefore could be useful for the development of 2D MSi_2N_4 based high-performance electronics.

Introduction

Two-dimensional (2D) semiconductors hold promise as channel materials for advancing nanoelectronics in the post-Moore era[1, 2], as their atomically thin thickness can effectively mitigate the short-channel effects, and their dangling-bond-free surfaces can preserve the carrier mobility even at monolayer limit[3-5]. Among many 2D semiconductors, monolayer MoS_2 and WS_2 have attracted tremendous interest, due to their high stability, appealing electronic properties and more importantly, their potential of large-scale growth.[6-11] 2D MoS_2 and WS_2 based electronic devices have been demonstrated, which show impressive performance.[12-15] It is noted that due to their extremely thin nature, these 2D semiconductors are vulnerable to external influences such as substrates or defects, leading to variation or degradation to the electronic properties.[16-19] 2D transition metal silicon nitrides (MSi_2N_4; M denotes Mo or W) are emerging semiconductor materials that might mitigate the above issue.[20] 2D MSi_2N_4 consists of septuple atomic layers, where metal cations that contribute dominantly to the valence and conduction band edges are sandwiched in the middle layer[20]. This indicates that the electronic properties of 2D MSi_2N_4 could be protected and less vulnerable to external influence[21, 22], which are highly desired for high-performance electronic device applications.

Various studies have suggested the promising application of 2D MSi_2N_4 as channel materials for 2D electronics[23, 24]. The performance of 2D MSi_2N_4-based electronic devices can be further improved by the integration of high-κ dielectrics. They can enhance electrostatic gate control on the channel, suppress charge impurity scattering, and reduce leakage current[25-27]. However, the high-performance integration of high-κ dielectrics into 2D electronics is challenging[28, 29]. This is partially due to high interface state density, which is formed when the high-κ dielectrics with

surface dangling bonds interfacing with 2D semiconductors that are dangling bond free. While tremendous effects have been paid to improve the integration of high-κ dielectrics on traditional 2D semiconductors such as MoS_2 or WS_2[30-41], such exploration on 2D MSi_2N_4 remains at the early stage. Among various high-κ dielectrics, silicon nitride (Si_3N_4) could be a promising candidate for the integration with 2D MSi_2N_4. This is because: (1) Si_3N_4 is the native high-κ dielectric of MSi_2N_4, which could be directly deposited on MSi_2N_4 using the similar growth process, enabling a much-simplified integration process; (2) There are no metallic elements in Si_3N_4, thus a weak interfacial interaction with 2D MSi_2N_4 can be expected; (3) Si_3N_4 is an excellent dielectric material with large band gap and high dielectric constant, which has been widely applied in current semiconductor technology and also the emerging 2D electronics[25, 42]. Thus, in this study, we explore the use of Si_3N_4 as the high-κ dielectric for 2D semiconductors MSi_2N_4 and propose interfacial hydrogenation to passivate the dangling bonds and improve the interface properties.

Method

All the calculations of this study were performed by using density-functional theory (DFT) based Vienna ab initio simulation package (VASP.6.1) with Perdew-Burke-Ernzerhof (PBE) exchange-correlational functional and the projector-augmented wave (PAW) potentials[43, 44]. The cutoff energy for plane wave expansion was set to 500 eV. The electronic and ionic convergence criteria were set to 10^{-5} eV and 0.01 eV/Å, respectively. For all slab models, a vacuum layer with a thickness of 15 Å was applied normally to the surfaces. For bulk β-Si_3N_4 and monolayer $MoSi_2N_4$ and WSi_2N_4, 6×6×15 and 12×12×1 Γ-centre *k*-point meshes were used to sample the first Brillouin zone, respectively. Based on these parameters, the lattice constants for β-Si_3N_4 are predicted to be

a=b=7.66 Å and c=2.92 Å. For the monolayer $MoSi_2N_4$ and WSi_2N_4, the calculated lattice constants are a=b=2.91 Å and a=b=2.92 Å, respectively. The calculated PBE band gaps for these materials are estimated at 4.24 eV for β-Si_3N_4, 1.72 eV for monolayer $MoSi_2N_4$, and 2.09 eV for monolayer WSi_2N_4. These values are in good agreement with the previous studies[20, 41, 45-48].

Results and Discussions

The interfaces between monolayer MSi_2N_4 and β-Si_3N_4(0001) were modelled by placing $3\sqrt{3}$ $\times 3\sqrt{3}$) monolayer MSi_2N_4 supercells on (2×2) Si_3N_4 (0001) supercell, where a small compressive strain of 1.31% and 1.11% was applied on Si_3N_4 (0001) to match $MoSi_2N_4$ and WSi_2N_4, respectively. As illustrated in Figure S1, such a small compressive strain does not bring any visible influence on the bandgap of Si_3N_4. The thickness of Si_3N_4(0001) was set to 5 atomic layers with the bottom surface passivated by hydrogen atoms. For interface models, Γ-centre 3×3×1 k-point meshes were used and van de Waals effects were considered using DFT-D3 method.[49] To verify the stability of the hydrogen passivated interface, ab initio molecular dynamics simulations were conducted, where the canonical ensemble (NVT) and the Nosé heat bath were applied for 6 ps with a time step of 1 fs. The energy barrier for hydrogen diffusion was evaluated using the nudged elastic band method.

To estimate the strength of the interfacial interaction between monolayer 2D MSi_2N_4 and Si_3N_4(0001), the absorption energy E_a and the charge density redistribution $\Delta\rho$ were calculated using the formula below:

$$E_a = \frac{E_i - E_{2D} - E_d}{A}, \quad (1)$$

and

$$\Delta\rho = \rho_i - \rho_{2D} - \rho_d, \quad (2)$$

respectively, where A stands for the interfacial area; E_i (ρ_i), E_{2D} (ρ_{2D}) and E_d (ρ_d) are total energy (charge density) of the interface, isolated monolayer MSi_2N_4 and Si_3N_4, respectively. The more negative adsorption energy indicates stronger interfacial interaction.

The most stable interface configuration of 2D $MoSi_2N_4/Si_3N_4$ (0001) was achieved by sliding 2D $MoSi_2N_4$ on the surface of Si_3N_4 (0001), in which the one with lowest energy is the most stable interface structure. The top view and side of the resulting structure are presented in Figure 1(a) and (b), in which the configuration is stabilised by maximising the interfacial bonding tendency. The optimized interfacial structure exhibits an interface spacing of 3.0 Å, at the range of van der Waals interaction, akin to the interfacial spacing observed between MoS_2 and Si_3N_4 (2.9 Å)[41]. This considerable interfacial distance implies a weak interaction between monolayer $MoSi_2N_4$ and Si_3N_4. The weak interfacial interaction is further supported by the calculated interface adsorption energy (-20.1 meV/Å^2), which is comparable to that of typical van der Waals systems such as bi-layer graphene or MoS_2.

The predicted interfacial properties of 2D $MoSi_2N_4/Si_3N_4$ (0001) are shown in Figure 1. As expected, the weak interfacial interaction results in promising interface performance. Figure 1(a) shows the interface charge density redistribution, which is weak and can only be noticeable at the small iso-surface values. In semiconductor devices, electron-hole puddles (spatial fluctuation of charge density distribution) are another characteristic feature to evaluate the device performance, as these carrier puddles materialise as scattering centres, leading to a reduction in carrier

mobility.[50] It turns out that the electron-hole puddles at the interface of $MoSi_2N_4/Si_3N_4$ are insignificant, as shown in Figure 1(b). We further examine the electronic structure of monolayer $MoSi_2N_4$ after the integration with Si_3N_4. As the projected density of states (PDOS) on the Mo layer (Figure 1 (c)) shows, the electronic properties of the 2D semiconductor $MoSi_2N_4$ nearly remain intact at the valence and conduction band edge, which are primarily contributed by the Mo d orbital. From Figure S2, we can further see that the integration of high-κ dielectric Si_3N_4 does not induce visible influence on the band gap of 2D $MoSi_2N_4$. This could be ascribed to: (1) the weak interfacial interaction between $MoSi_2N_4$ and Si_3N_4, and (2) the unique structure of $MoSi_2N_4$, in which the sandwiched Mo layer is well protected and less influenced by the Si_3N_4. These attributes are highly desired for device applications as the integration of the high-κ dielectric does not affect the electronic properties of the 2D semiconductor.

It is also noted that there are dangling bonds at Si_3N_4 surface, which introduce mid-gap states and couple with the orbitals of the nearest neighbouring N atom in the $MoSi_2N_4$, as shown in Figure 1(d) and (e). This leads to high interface state density and diminished band offsets between high-κ dielectric Si_3N_4 and 2D semiconductor $MoSi_2N_4$. The high interface state density will lead to reduced carrier mobility and on/off ratio in the channel, less efficient gate-control, and ultimately, deterioration in device performance. On the other hand, the small band offsets lead to a large leakage current[25].

Since the aforementioned issues are due to the dangling bonds at $Si_3N_4(0001)$ surface, one natural solution is to passivate these dangling bonds using interfacial engineering techniques[51]. Interfacial hydrogenation has been reported that can effectively passivate the dangling bonds of

Si_3N_4[41, 52]. Therefore, we also employed hydrogenation to passivate the dangling bonds. We find that this interfacial hydrogenation can further improve the interface performance between Si_3N_4 and $MoSi_2N_4$. Firstly, the passivated interface shows weaker interfacial interaction, compared to the interface without the passivation, as supported by the calculated adsorption energy in Figure 2(a). Secondly, the charge redistribution and electron-hole puddles at the passivated interface are further reduced, as shown in Figure 2(b) and (c). Thirdly, the passivated interface removes the mid-gap states in Si_3N_4 and decouples the orbital hybridization between Si_3N_4 and $MoSi_2N_4$, leading to sizable band offsets. As the PDOSs shown in Figure 2(d), the conduction and valence band offsets are estimated to be 2. 45 eV and 0.59 eV at PBE level, respectively. The conduction band offset is large enough to minimise electron tunnelling for *n*-channel devices.

For the interfacial hydrogenation, it is highly desired that the treatment process is capable of only passivating the dangling bonds at the high-κ dielectric surface and not affecting the 2D semiconductor. This can be evaluated by the adsorption energy difference for hydrogen atom adsorbed at the Si_3N_4 and $MoSi_2N_4$. If the adsorption energy of hydrogen atom at the surface is negative, it indicates an energetically favourable hydrogenation process towards the surface. In contrast, if the adsorption energy is positive, it indicates that the hydrogenation is energetically unfavourable towards the surface and would lead to minimized effects to the surface. In Figure 3(a) summarises the calculated hydrogen adsorption energy at the surface of Si_3N_4 and $MoSi_2N_4$, respectively. The adsorption energy for hydrogen atoms at 2D $MoSi_2N_4$ is 1.94 eV. This very positive adsorption energy indicates that $MoSi_2N_4$ surface is inert to hydrogen adsorption, similar to that MoS_2 surface.[53] In contrast, the hydrogen adsorption at Si_3N_4 surface is energetically favourable. As shown in Fig. 3(a), the adsorption energy for hydrogen atoms adsorbed at the surface N and Si sites with the dangling bonds is -0.76 eV and -1.43 eV, respectively. Thus, it is

expected that the interfacial hydrogenation process can only passivate the dangling bonds at the Si_3N_4 surface and will not affect 2D $MoSi_2N_4$ due to this thermodynamic constrain. We also find that the hydrogenated interface is thermally stable. Figure 3(b) and (c) show that the variation of Si-H bonds is within 0.07 Å and the hydrogen atoms remains stable at the Si_3N_4 surface during the 6 ps MD simulation at the temperature of 800 K. Further calculation shown in Figure 3(d) suggests that a high energy barrier of 2.6 eV is required for hydrogen atom diffused from Si_3N_4 surface to the second layer of Si_3N_4, confirming that the hydrogenation process is also kinetically stable at the Si_3N_4 surface, and can minimize the formation of undesired interstitial defects in Si_3N_4. All these results evidence that interfacial hydrogenation is an effective method to improve the interface properties and can minimize the detrimental effects to both MoS_2iN_4 and Si_3N_4.

In addition to 2D $MoSi_2N_4$, monolayer WSi_2N_4 has also been synthesised in the experiment. Next, we examine the interface properties of high-κ dielectric Si_3N_4 and 2D WSi_2N_4. It turns out that the interaction between 2D WSi_2N_4 and Si_3N_4 is weak, which can be seen from the small adsorption energy (-20.43 eV/Å^2), insignificantly charge redistribution (see Figure 4(a)), and preserved electronic properties of 2D WSi_2N_4 near the Fermi level (see Figure 4(b)). However, the dangling bonds from Si_3N_4 also introduces mid-gap states, which couples with those of WSi_2N_4, leading to insignificant band offset, as shown in Figure 4(c). In this regard, interfacial hydrogenation was further employed to passivate the dangling bonds. As shown in Figure 3(a), the interfacial hydrogenation is also only energetically favourable towards the dangling bonds at the Si_3N_4 surface. The interfacial hydrogenation on the Si_3N_4 surface further weakens the interfacial interaction, where the calculated adsorption is about -19.13 eV/Å^2. After the hydrogenation, the interface between 2D WSi_2N_4 and Si_3N_4 shows improved performance. As shown in Figure 4(b), the charge

density redistribution is insignificant, compared to that of the one without the passivation (Figure 4(a)). Notably, the passivation removes the mid-gap states and decouples the orbital hybridization, resulting in the noticeable band offsets between the 2D semiconductor WSi_2N_4 and the high-κ dielectric Si_3N_4. The interface now exhibits asymmetric type-II band offsets with a large conduction band offset (>2.04 eV). Therefore, these results suggest that the selective hydrogenation passivation methodology not only improves the electronic properties for the interface between $MoSi_2N_4$ and Si_3N_4, but also enhances the interface performance between WSi_2N_4 and Si_3N_4. In experiment, the interfacial hydrogenation could be realized by depositing Si_3N_4 at the elevated temperature assisted with atomic hydrogen source. Besides, we are aware that current PBE calculations leads to underestimated band gaps of 2D MSi_2N_4 and Si_3N_4, as well as the band offsets between them. These, however, do not affect the validity of the results. Further HSE calculations increase the band gaps approaching experimental values, but they still lead to the asymmetric band offsets, in which the VBO remains below 1 eV.

Conclusion

In conclusion, based on in-depth first-principles calculation, we report the interface properties between silicon nitride and 2D semiconductors $MoSi_2N_4$ and WSi_2N_4. We reveal that hydrogenation process is a desired interface engineering technique, which can occur spontaneously, and effectively passivate the dangling bonds at the Si_3N_4 surface, without bringing detrimental effects to both Si_3N_4 and the 2D semiconductors. The hydrogen passivated interface shows much-improved interface performance, as evidenced by the diminished interface states, increased band offsets, and well-preserved electronic properties of the 2D semiconductors. These findings highlight that Si_3N_4 is a promising native high-κ dielectric for 2D semiconductors $MoSi_2N_4$ and

WSi_2N_4 with a much-simplified integration process. Our work affirms the effectiveness and generality of the proposed selective hydrogenation approach for a broad range of high-κ dielectrics/2D semiconductor interfaces, thereby bolstering advancements in 2D electronics.

AUTHOR DECLARATIONS

Conflict of Interest

The authors have no conflicts to disclose.

Acknowledgement

M.Y. acknowledges the funding support from the National Key R&D Program of the Ministry of Science and Technology of China (project number: 2022YFA1203804), the Hong Kong Polytechnic University (project number: ZE2F, CE04, and ZE2X) and PolyU RCNN (Project No.: CE0H), and Research Grants Council, Hong Kong (project number: F-PP8T). We thank National Supercomputing Centre, Singapore for providing the computing resource.

REFERENCES

[1] M.Y. Li, S.K. Su, H.P. Wong, L.J. Li, How 2D semiconductors could extend Moore's law, Nature, 567 (2019) 169-170.

[2] G. Fiori, F. Bonaccorso, G. Iannaccone, T. Palacios, D. Neumaier, A. Seabaugh, S.K. Banerjee, L. Colombo, Electronics based on two-dimensional materials, Nature nanotechnology, 9 (2014) 768-779.

[3] S. Wang, X. Liu, P. Zhou, The Road for 2D Semiconductors in the Silicon Age, Adv Mater, 34 (2022) e2106886.

[4] Y. Liu, X. Duan, H.-J. Shin, S. Park, Y. Huang, X. Duan, Promises and prospects of two-dimensional transistors, Nature, 591 (2021) 43-53.

[5] M. Chhowalla, D. Jena, H. Zhang, Two-dimensional semiconductors for transistors, Nature Reviews Materials, 1 (2016) 1-15.

[6] K.F. Mak, C. Lee, J. Hone, J. Shan, T.F. Heinz, Atomically thin MoS 2: a new direct-gap semiconductor, Physical review letters, 105 (2010) 136805.

[7] K. Kang, S. Xie, L. Huang, Y. Han, P.Y. Huang, K.F. Mak, C.-J. Kim, D. Muller, J. Park, High-mobility three-atom-thick semiconducting films with wafer-scale homogeneity, Nature, 520 (2015) 656-660.

[8] M. Yang, J.W. Chai, M. Callsen, J. Zhou, T. Yang, T.T. Song, J.S. Pan, D.Z. Chi, Y.P. Feng, S.J. Wang, Interfacial interaction between HfO2 and MoS2: From thin films to monolayer, The Journal of Physical Chemistry C, 120 (2016) 9804-9810.

[9] J. Chai, S. Tong, C. Li, C. Manzano, B. Li, Y. Liu, M. Lin, L. Wong, J. Cheng, J. Wu, Memory Devices: MoS2/Polymer Heterostructures Enabling Stable Resistive Switching and Multistate Randomness (Adv. Mater. 42/2020), Advanced Materials, 32 (2020) 2070317.

[10] Q.H. Wang, K. Kalantar-Zadeh, A. Kis, J.N. Coleman, M.S. Strano, Electronics and optoelectronics of two-dimensional transition metal dichalcogenides, Nature nanotechnology, 7 (2012) 699-712.

[11] G.-B. Liu, D. Xiao, Y. Yao, X. Xu, W. Yao, Electronic structures and theoretical modelling of two-dimensional group-VIB transition metal dichalcogenides, Chemical Society Reviews, 44 (2015) 2643-2663.

[12] H.K. Ng, D. Xiang, A. Suwardi, G. Hu, K. Yang, Y. Zhao, T. Liu, Z. Cao, H. Liu, S. Li, Improving carrier mobility in two-dimensional semiconductors with rippled materials, Nature Electronics, 5 (2022) 489-496.

[13] F. Wu, H. Tian, Y. Shen, Z. Hou, J. Ren, G. Gou, Y. Sun, Y. Yang, T.-L. Ren, Vertical MoS2 transistors with sub-1-nm gate lengths, Nature, 603 (2022) 259-264.

[14] S.B. Desai, S.R. Madhvapathy, A.B. Sachid, J.P. Llinas, Q. Wang, G.H. Ahn, G. Pitner, M.J. Kim, J. Bokor, C. Hu, MoS2 transistors with 1-nanometer gate lengths, Science, 354 (2016) 99-102.

[15] B. Radisavljevic, A. Radenovic, J. Brivio, V. Giacometti, A. Kis, Single-layer MoS2 transistors, Nature nanotechnology, 6 (2011) 147-150.

[16] Z. Qiu, M. Trushin, H. Fang, I. Verzhbitskiy, S. Gao, E. Laksono, M. Yang, P. Lyu, J. Li, J. Su, Giant gate-tunable bandgap renormalization and excitonic effects in a 2D semiconductor, Science advances, 5 (2019) eaaw2347.

[17] M.M. Ugeda, A.J. Bradley, S.-F. Shi, F.H. Da Jornada, Y. Zhang, D.Y. Qiu, W. Ruan, S.-K. Mo, Z. Hussain, Z.-X. Shen, Giant bandgap renormalization and excitonic effects in a monolayer transition metal dichalcogenide semiconductor, Nature materials, 13 (2014) 1091-1095.
[18] H.-P. Komsa, A.V. Krasheninnikov, Effects of confinement and environment on the electronic structure and exciton binding energy of MoS 2 from first principles, Physical Review B, 86 (2012) 241201.
[19] Y. Yang, T. Song, X. Zhang, Y. Zhao, J. Chai, Z. Cheng, X. Huang, H. Zhang, W. Zhu, M. Yang, Substrate mediated electronic and excitonic reconstruction in a MoS 2 monolayer, Journal of Materials Chemistry C, 8 (2020) 11778-11785.
[20] Y.-L. Hong, Z. Liu, L. Wang, T. Zhou, W. Ma, C. Xu, S. Feng, L. Chen, M.-L. Chen, D.-M. Sun, Chemical vapor deposition of layered two-dimensional MoSi2N4 materials, Science, 369 (2020) 670-674.
[21] Y. Wu, Z. Tang, W. Xia, W. Gao, F. Jia, Y. Zhang, W. Zhu, W. Zhang, P. Zhang, Prediction of protected band edge states and dielectric tunable quasiparticle and excitonic properties of monolayer MoSi2N4, npj Computational Materials, 8 (2022) 129.
[22] J. Zhang, Y. Xia, L. Peng, Y. Zhang, B. Li, L. Shu, Y. Cen, J. Zhuang, H. Zhu, P. Zhan, Ultra-Confined Phonon Polaritons and Strongly Coupled Microcavity Exciton Polaritons in Monolayer MoSi2N4 and WSi2N4, Advanced Science, DOI (2024) 2307691.
[23] K. Nandan, B. Ghosh, A. Agarwal, S. Bhowmick, Y.S. Chauhan, Two-dimensional MoSi 2 N 4: An excellent 2-D semiconductor for field-effect transistors, IEEE Transactions on Electron Devices, 69 (2021) 406-413.
[24] L. Cao, G. Zhou, Q. Wang, L. Ang, Y.S. Ang, Two-dimensional van der Waals electrical contact to monolayer MoSi2N4, Applied Physics Letters, 118 (2021).
[25] J. Robertson, High dielectric constant gate oxides for metal oxide Si transistors, Reports on Progress in Physics, 69 (2005) 327.
[26] B. Wang, W. Huang, L. Chi, M. Al-Hashimi, T.J. Marks, A. Facchetti, High-k gate dielectrics for emerging flexible and stretchable electronics, Chemical reviews, 118 (2018) 5690-5754.
[27] D. Jena, A. Konar, Enhancement of carrier mobility in semiconductor nanostructures by dielectric engineering, Physical review letters, 98 (2007) 136805.
[28] S. Das, A. Sebastian, E. Pop, C.J. McClellan, A.D. Franklin, T. Grasser, T. Knobloch, Y. Illarionov, A.V. Penumatcha, J. Appenzeller, Transistors based on two-dimensional materials for future integrated circuits, Nature Electronics, 4 (2021) 786-799.
[29] Y.Y. Illarionov, T. Knobloch, M. Jech, M. Lanza, D. Akinwande, M.I. Vexler, T. Mueller, M.C. Lemme, G. Fiori, F. Schwierz, Insulators for 2D nanoelectronics: the gap to bridge, Nature Communications, 11 (2020) 3385.
[30] L.H. Li, E.J. Santos, T. Xing, E. Cappelluti, R. Roldán, Y. Chen, K. Watanabe, T. Taniguchi, Dielectric screening in atomically thin boron nitride nanosheets, Nano letters, 15 (2015) 218-223.
[31] S. Yang, K. Liu, Y. Xu, L. Liu, H. Li, T. Zhai, Gate Dielectrics Integration for 2D Electronics: Challenges, Advances, and Outlook, Advanced Materials, 35 (2023) 2207901.
[32] A.K. Geim, I.V. Grigorieva, Van der Waals heterostructures, Nature, 499 (2013) 419-425.
[33] T. Knobloch, B. Uzlu, Y.Y. Illarionov, Z. Wang, M. Otto, L. Filipovic, M. Waltl, D. Neumaier, M.C. Lemme, T. Grasser, Improving stability in two-dimensional transistors with amorphous gate oxides by Fermi-level tuning, Nature Electronics, 5 (2022) 356-366.

[34] Y.Y. Illarionov, A.G. Banshchikov, D.K. Polyushkin, S. Wachter, T. Knobloch, M. Thesberg, L. Mennel, M. Paur, M. Stöger-Pollach, A. Steiger-Thirsfeld, Ultrathin calcium fluoride insulators for two-dimensional field-effect transistors, Nature Electronics, 2 (2019) 230-235.
[35] J.-K. Huang, Y. Wan, J. Shi, J. Zhang, Z. Wang, W. Wang, N. Yang, Y. Liu, C.-H. Lin, X. Guan, High-κ perovskite membranes as insulators for two-dimensional transistors, Nature, 605 (2022) 262-267.
[36] A.J. Yang, K. Han, K. Huang, C. Ye, W. Wen, R. Zhu, R. Zhu, J. Xu, T. Yu, P. Gao, Van der Waals integration of high-κ perovskite oxides and two-dimensional semiconductors, Nature Electronics, 5 (2022) 233-240.
[37] K. Liu, B. Jin, W. Han, X. Chen, P. Gong, L. Huang, Y. Zhao, L. Li, S. Yang, X. Hu, A wafer-scale van der Waals dielectric made from an inorganic molecular crystal film, Nature Electronics, 4 (2021) 906-913.
[38] Y. Xu, T. Liu, K. Liu, Y. Zhao, L. Liu, P. Li, A. Nie, L. Liu, J. Yu, X. Feng, Scalable integration of hybrid high-κ dielectric materials on two-dimensional semiconductors, Nature Materials, 22 (2023) 1078-1084.
[39] W. Li, J. Zhou, S. Cai, Z. Yu, J. Zhang, N. Fang, T. Li, Y. Wu, T. Chen, X. Xie, Uniform and ultrathin high-κ gate dielectrics for two-dimensional electronic devices, Nature Electronics, 2 (2019) 563-571.
[40] P. Luo, C. Liu, J. Lin, X. Duan, W. Zhang, C. Ma, Y. Lv, X. Zou, Y. Liu, F. Schwierz, Molybdenum disulfide transistors with enlarged van der Waals gaps at their dielectric interface via oxygen accumulation, Nature Electronics, 5 (2022) 849-858.
[41] Y. Yang, T. Yang, T. Song, J. Zhou, J. Chai, L.M. Wong, H. Zhang, W. Zhu, S. Wang, M. Yang, Selective hydrogenation improves interface properties of high-k dielectrics on 2D semiconductors, Nano Research, 15 (2022) 4646-4652.
[42] M. Yang, J. Chai, Y. Wang, S. Wang, Y. Feng, Interfacial properties of silicon nitride grown on epitaxial graphene on 6H-SiC substrate, The Journal of Physical Chemistry C, 116 (2012) 22315-22318.
[43] G. Kresse, J. Furthmüller, Efficiency of ab-initio total energy calculations for metals and semiconductors using a plane-wave basis set, Computational materials science, 6 (1996) 15-50.
[44] G. Kresse, J. Furthmüller, Efficient iterative schemes for ab initio total-energy calculations using a plane-wave basis set, Physical review B, 54 (1996) 11169.
[45] Q. Wang, L. Cao, S.-J. Liang, W. Wu, G. Wang, C.H. Lee, W.L. Ong, H.Y. Yang, L.K. Ang, S.A. Yang, Efficient Ohmic contacts and built-in atomic sublayer protection in MoSi2N4 and WSi2N4 monolayers, npj 2D Materials and Applications, 5 (2021) 71.
[46] S. Li, W. Wu, X. Feng, S. Guan, W. Feng, Y. Yao, S.A. Yang, Valley-dependent properties of monolayer MoSi 2 N 4, WSi 2 N 4, and MoSi 2 As 4, Physical Review B, 102 (2020) 235435.
[47] M. Yang, S. Wang, Y. Feng, G. Peng, Y. Sun, Electronic structure of germanium nitride considered for gate dielectrics, Journal of applied physics, 102 (2007).
[48] Y. Yang, H. Lyu, Z. Li, Z. Yu, Y. Huang, Z. Ning, Two-dimensional Janus SnS/MoSi2N4 structure for high-efficiency photocatalytic splitting, Computational Materials Science, 234 (2024) 112781.
[49] S. Grimme, S. Ehrlich, L. Goerigk, Effect of the damping function in dispersion corrected density functional theory, Journal of computational chemistry, 32 (2011) 1456-1465.

[50] J. Martin, N. Akerman, G. Ulbricht, T. Lohmann, J.v. Smet, K. Von Klitzing, A. Yacoby, Observation of electron–hole puddles in graphene using a scanning single-electron transistor, Nature physics, 4 (2008) 144-148.
[51] S. Ashok, Research in Hydrogen Passivation of Defects and Impurities in Silicon: Final Report, 2 May 2000-2 July 2003, National Renewable Energy Lab.(NREL), Golden, CO (United States), 2004.
[52] M. Yang, R. Wu, W. Deng, L. Shen, Z. Sha, Y. Cai, Y. Feng, S. Wang, Electronic structures of β-Si3N4 (0001)/Si (111) interfaces: Perfect bonding and dangling bond effects, Journal of Applied Physics, 105 (2009).
[53] T. Yang, Y. Bao, W. Xiao, J. Zhou, J. Ding, Y.P. Feng, K.P. Loh, M. Yang, S.J. Wang, Hydrogen evolution catalyzed by a molybdenum sulfide two-dimensional structure with active basal planes, ACS applied materials & interfaces, 10 (2018) 22042-22049.

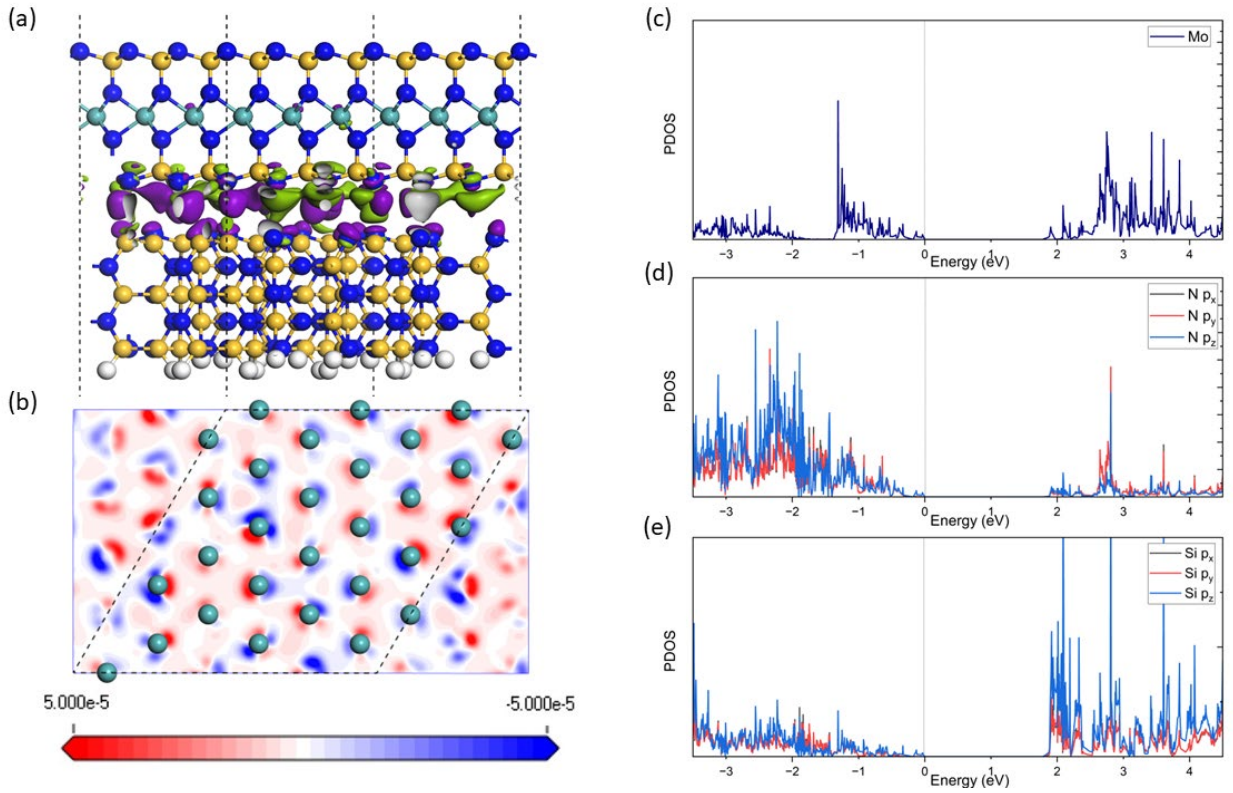

Figure 1. Interfacial structures and properties between monolayer $MoSi_2N_4$ and Si_3N_4 (0001). (a) Side and (b) top views of the most stable configuration for the interfacial structures, in which the green and purple colour in (a) denotes the depleted and accumulated charge density visualised by an iso-surface value of 1.0×10^{-4} e/Å^3, respectively. The red and blue colours in (b) denote the charge puddles formed on the Mo plane by an iso-surface value of 5×10^{-5} e/Å^2. (c)-(e) The projected density of states on Mo, N, and Si, respectively.

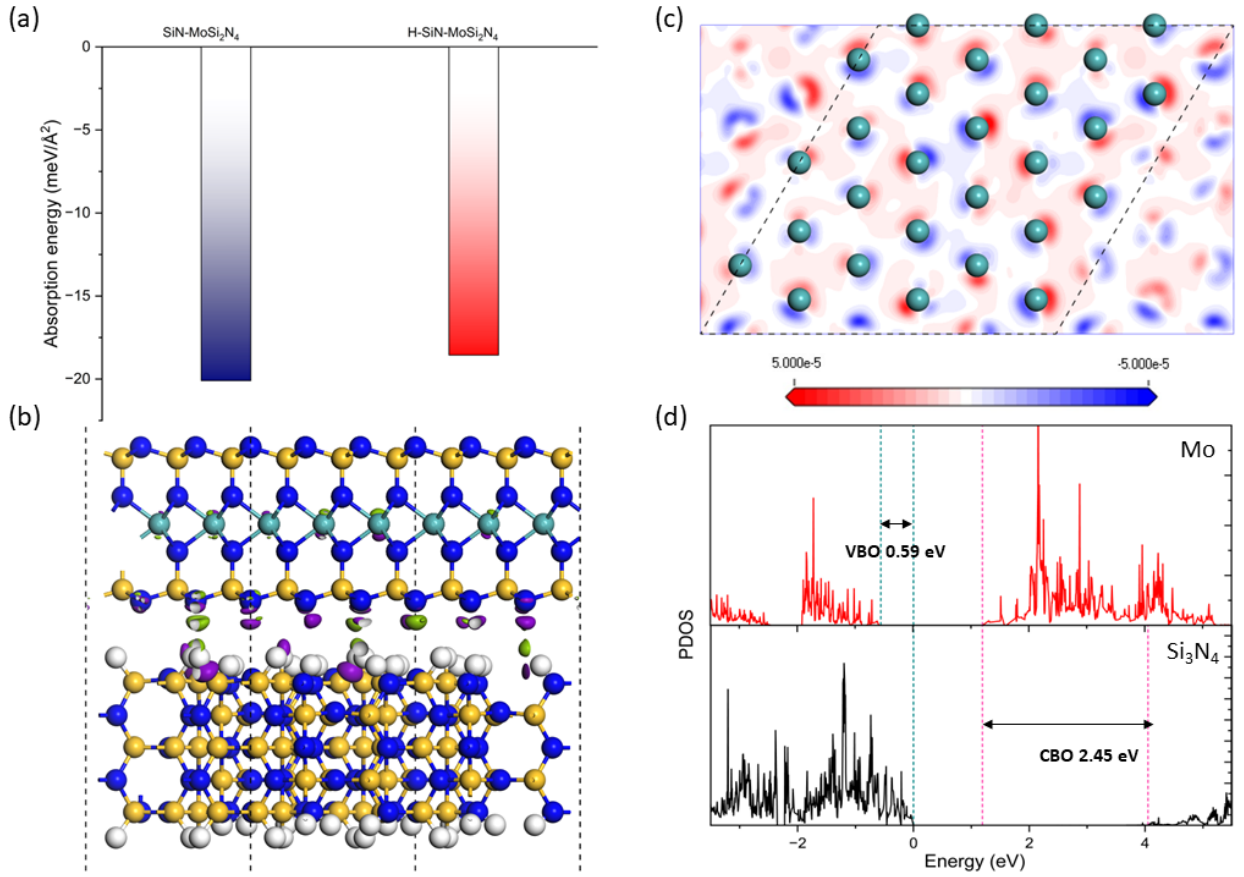

Figure 2. Interfacial properties of monolayer $MoSi_2N_4/Si_3N_4$ with the hydrogenation treatment. (a) The absorption energy for the interfaces with/without the hydrogenation. (b) The side and (c) top views of the hydrogen-passivated interfacial structure. The green and purple colours in (b) denote the depleted and accumulated charge density visualised by an iso-surface value of 1.0×10^{-4} e/Å^3, respectively. The red and blue colour in (c) denotes the electron-hole puddle distribution on the Mo plane by an iso-surface value of 5×10^{-5} e/Å^2. (d) The PDOS of the interface projected on the Mo layer and the middle layer of Si_3N_4 (0001), respectively, showing the valence and conduction band offsets.

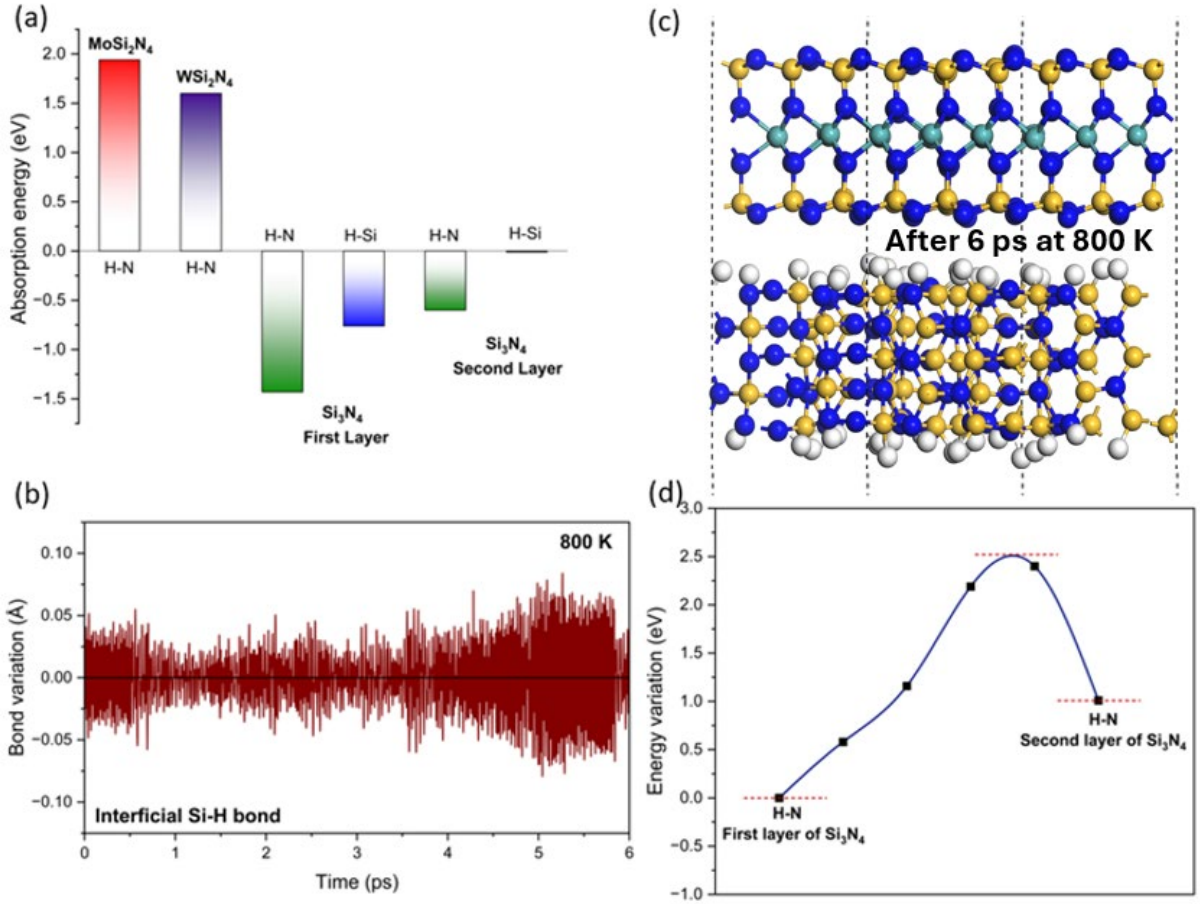

Figure 3. The thermodynamic and kinetic stability of the hydrogenated interface. (a) The absorption energy for hydrogen atom adsorbed at Si_3N_4, $MoSi_2N_4$ and WSi_2N_4 surface and at the second layer of Si_3N_4. (b) The interfacial Si-H bond variation during the molecular dynamic (MD) simulation at the temperature of 800 K. (c) The side view of the atomic structure for the passivated interface after 6 ps MD simulation. (d) The energy barrier for a hydrogen atom diffused from Si_3N_4 surface to the second layer of Si_3N_4.

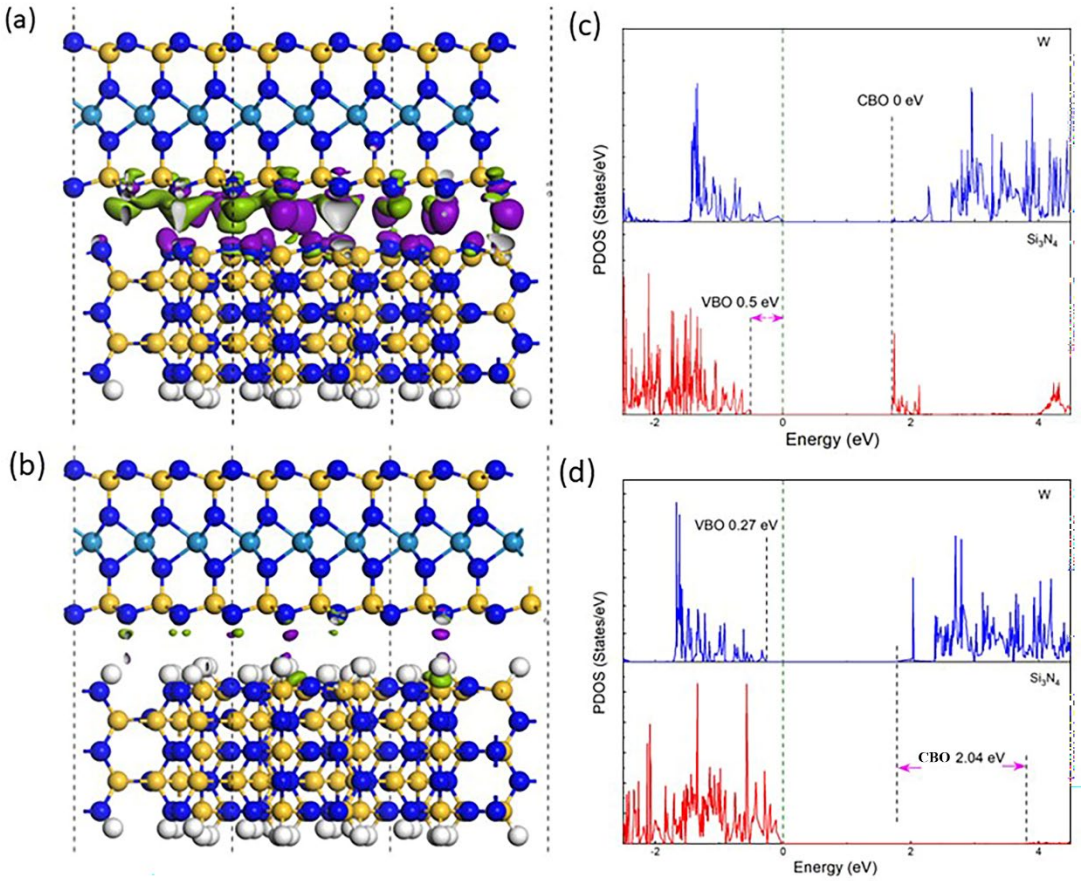

Figure 4. Interfacial structures and properties between monolayer WSi_2N_4 and Si_3N_4 before and after passivation processes. The interfacial charge transfer between WSi_2N_4 and Si_3N_4 before (a) and after (b) hydrogen passivation, in which the green and purple dots indicate the depleted and accumulated charge density visualised by an iso-surface value of 5×10^{-4} e/Å^3, respectively. (c) and (d) The projected density of states (PDOS) on both the middle layers of Si_3N_4 and W layers before and after hydrogen passivation, respectively, where the Fermi level is set to 0 eV.